

THE 4TH INTERNATIONAL CONFERENCE ON ALUMINUM ALLOYS

PRECIPITATION IN Al-Li-Zn TERNARY ALLOYS

A. Yamamoto¹, H. Tsubakino¹ and R. Nozato²

1. Department of Materials Science and Engineering, Faculty of Engineering, Himeji Institute of Technology, 2167 Shosha, Himeji 671-22, Japan

2. Emeritus Professor, Himeji Institute of Technology

Abstract

Precipitation in Al-Li-Zn alloys has been investigated by hardness measurement, resistivity and specific heat measurements, and by transmission electron microscopic observations. Resistivity increased during aging at the temperatures lower than 348 K without any incubation period then decreased, while resistivity decreased at higher temperatures. On the specific heat versus temperature curves for the specimens, three heat absorptions appeared, which are considered to be due to redissolution of the equilibrium phase T ((Al,Zn)₂Li), metastable phase δ' (Al₃Li) and the precursor to the δ' phase (δ''). The precipitation sequence of the Al-Li-Zn alloy is considered as follows: Supersaturated α solid solution $\rightarrow \delta'' \rightarrow \delta' \rightarrow T$. The δ' and thin plate T phase contributed to age hardening. It is considered that the δ'' has a Li₂-like crystal structure.

Introduction

The effects of addition of the third element on the precipitation in Al-Li alloys have been investigated in order to improve the mechanical properties of the alloys. However, there are few studies on the effects of zinc addition (1,2), while it is common element for aluminum alloys. Jones and Das (1) reported that the addition of zinc did not result in substantial improvement of mechanical properties for the relatively low zinc content alloy (1.34 mass%). Recently, the effect of zinc addition on strengthening the commercial alloys for welding usage was reported (3), in which the mechanism of increasing the strength was not clearly explained.

Elemental precipitation sequence in Al-Li-Zn ternary alloys is investigated in the present study.

Experimental Procedures

High purity aluminum (99.99%), zinc (99.99%) and lithium (99.9%) were used to prepare three Al-Li-Zn ternary alloys, which were melted in high purity alumina crucible under argon atmosphere, then cast into iron mould. The alloys were homogenized at 803 K for 170 ks. Chemical composition of these alloys are listed in Table I. Specimens were solution heat treated at 803 K for 3.6 ks

Table I. Chemical Compositions of the Alloys

Alloy	Li*	Zinc*
I	1.7	8.5
II	1.7	4.0
III	2.0	4.0

* in mass%

under argon atmosphere, quenched in iced water and then aged at the temperatures in a range of 303 to 573 K.

Micro-Vickers hardness was measured with 0.98 N load. Specific heat (S) versus temperature (T) curves were obtained by means of adiabatic type of calorimeter under the heating rate of about 0.033 K/s. Measurements of resistivity (ρ) were carried out by potentiometric method. Specimens were dipped in liquid nitrogen during measuring. Transmission electron microscopy (TEM) and X-ray diffraction techniques (XRD) were used to identify the precipitates. Since the threshold voltage for electron irradiation damage for aluminum is about 150 kV (4), TEM observations were performed under an accelerating voltage of 100 kV using JEOL JEM-2010.

Results

Hardness Change

Changes in hardness with aging time in the Al-1.7%Li-8.5%Zn (Alloy I) and Al-1.7%Li-4.0%Zn (Alloy II) are shown in Figures 1 and 2, respectively.

On the Alloy I, two-stage increase in hardness can be seen at 383 K and 423 K aging (Figure 1). On the Alloy II, such a two-stage increase did not appear (Figure 3).

Since the hardness change on the Alloy II and Alloy III are similar each other, the results on the Alloy I and Alloy II are mainly referred hereafter.

S-T Curves

Typical examples of the S-T curves for the Alloy I are shown in Figure 3. On the S-T curve of the as quenched specimen, heat absorptions B, C and D and heat evolution Q appear. Heat evolution is due to precipitation and heat absorption

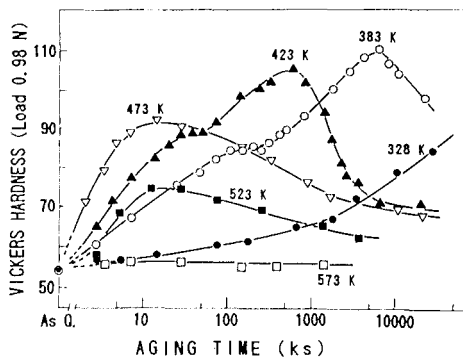


Figure 1. Changes in hardness in the Alloy I (Al-1.7Li-8.5Zn).

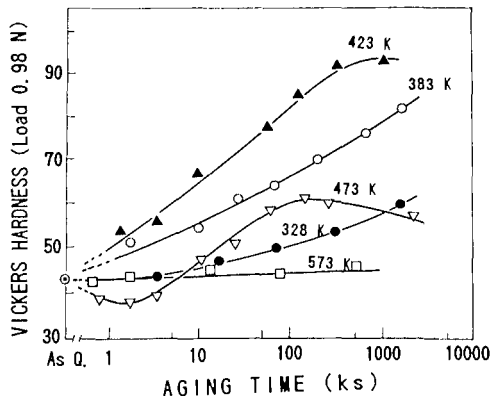


Figure 2. Changes in hardness in the Alloy II (Al-1.7Li-4.0Zn).

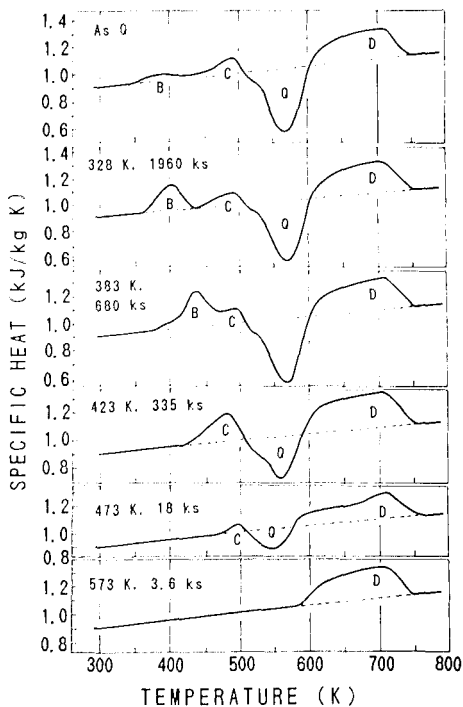


Figure 3. S-T curves for the Alloy I.

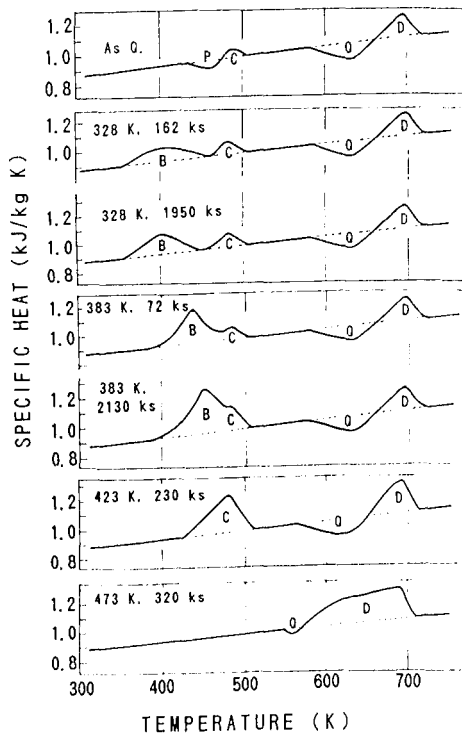


Figure 4. S-T curves for the Alloy II.

is due to redissolution. Heat absorption D has the highest peak temperature (T_p) in the present study, therefore, it is considered to be due to redissolution of the equilibrium phase and heat evolution Q is due to precipitation of the phase during measuring, and B and C are due to redissolution of metastable phases.

The areas surrounded by the S-T curve (solid line) and the base line (broken line) have a dimension of energy (kJ/kg) and correspond to the amount of precipitates in concerned with the heat evolution or heat absorption. The energy of heat evolution Q ([Q]) is about equal to that of heat absorption D ([D]), which means that only metastable phases existed in the as quenched state. Energy [B] increases with aging, and T_p of B becomes to be higher. On the S-T curve of the specimen aged at 423 K for 335 ks, B disappears and [C] increases, and also [D] becomes to be larger than [Q]. Aging at 473 K results in decrease of [C] and increase of [D]. Only D appears on the S-T curve of the specimen aged at 573 K for 3.6 ks. On the Alloy II, similar heat reactions can be seen on the S-T curves as shown in Figure 5, except the fact that the metastable phases are not formed in the as quenched specimen.

Energy [B+C] and [D-Q] are corresponding to the amount of the precipitates of the metastable and stable phases formed during aging, respectively. In Figures 6 and 7, they are plotted against aging time for the Alloy I and II, respectively. In the Alloy I, precipitation of the stable phase starts after about 500 ks at 383 K, and about 30 ks at 423 K. On the aging at 473 K, the stable phase seems to be formed from the beginning of aging. In the Alloy II, the precipitation of the stable phase occurs after about 200 ks at 423 K and about 50 ks at 473 K.

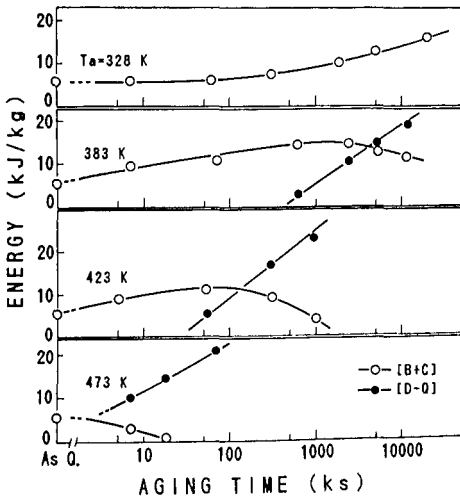


Figure 5. Change in energy [B+C] and [D-Q] in the Alloy I.

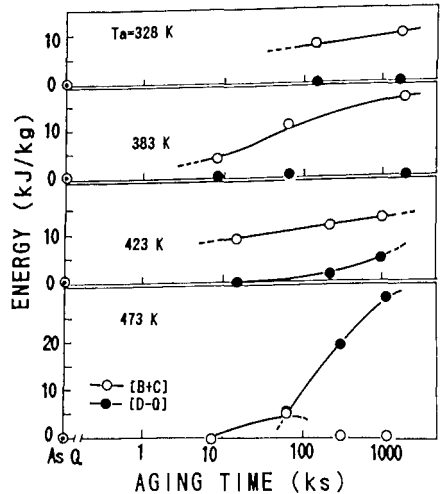


Figure 6. Change in energy [B+C] and [D-Q] in the Alloy II.

It is known that there are two ternary compounds in the Al-Li-Zn system, that is, $\text{Li}_{26}\text{Al}_6(\text{Zn}_{1-x}\text{Al}_x)_4$ and LiZn_3Al (5). The former was referred as $(\text{Al,Zn})_2\text{Li}$ (T phase) by Mondolfo (6), which has a cubic crystal structure with $a_0=1.4$ nm. The XRD investigations showed that the stable phases formed in the Alloy I and Alloy II were T phase and the metastable phases in these alloys were δ' (Al_3Li) phase. Any other phase was not detected.

Resistivity Change

Resistivity measurements were carried out on the Alloy II. Changes in resistivity during aging at 303 to 348 K are shown in Figure 7 and those aged at 383 to 473 K are shown in Figure 8. ρ_0 is the resistivity of the as quenched specimen and ρ is that of the aged specimen.

Resistivity increases without incubation period and then decreases at low temperatures (Figure 7), which is similar to the resistivity change in the Al-Li binary alloy (7). In the aging at 383 K, resistivity decreases in a single stage and at 423 and 473 K aging, resistivity decreases in two-stage (Figure 8). Decrease in the second stage begins after about 200 ks at 423 K aging and about 50 ks at 473 K aging, which are close to the periods of increasing the energy $[D-Q]$ at these temperatures (see Figure 6).

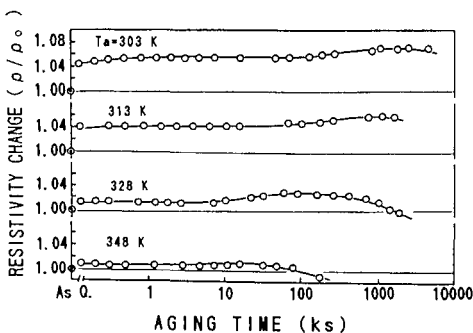


Figure 7. Change in resistivity in the Alloy II aging at 303 to 348 K.

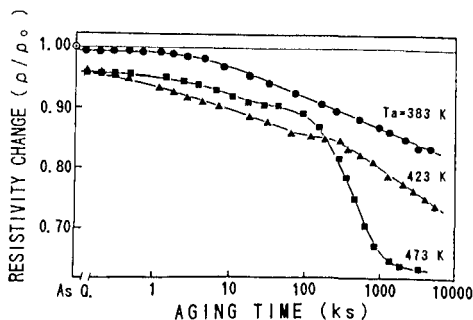


Figure 8. Change in resistivity in the Alloy II aging at 383 to 473 K.

TEM observation

Figure 9 shows the results of TEM observations for the Alloy I. In the specimen aged at 328 K for 1782 ks, distorted spherical shaped precipitates can be seen in (a) with Li_2 type super lattice reflections in (b), which are considered to be the δ' phase. Thin plate like precipitates are observed in the specimen aged at 423 K for 187 ks in (c), which is identified as T phase from the analysis of the diffraction pattern in (d). The precipitates T is formed along $\{111\}$ planes of the matrix α . With proceeding the aging at 473 K, only T phase becomes to be observed (f).

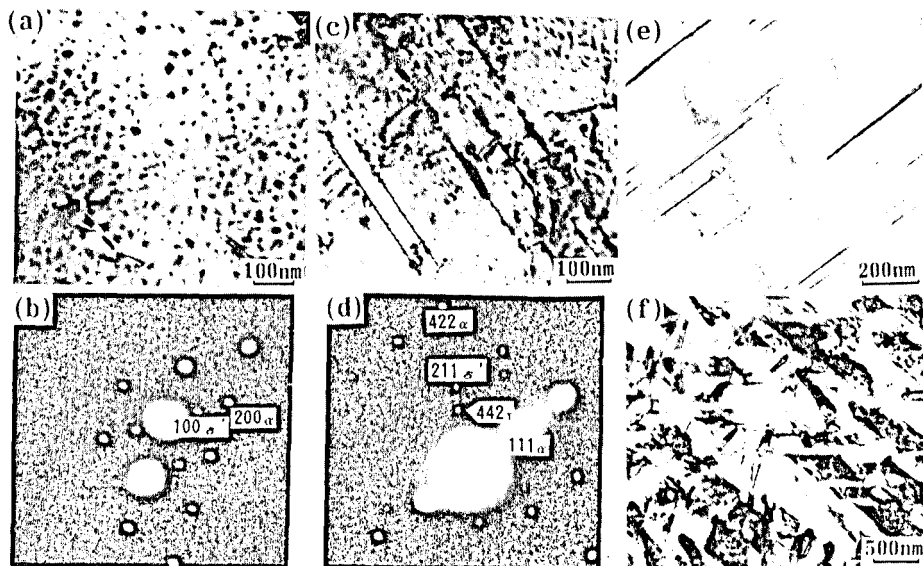


Figure 9. TEM micrographs and diffraction patterns of the Alloy I aged at 328 K for 1782 ks:(a) and (b), at 423 K for 187 ks:(c) and (d), at 473 K for 0.36 ks:(e) and 68 ks:(f).

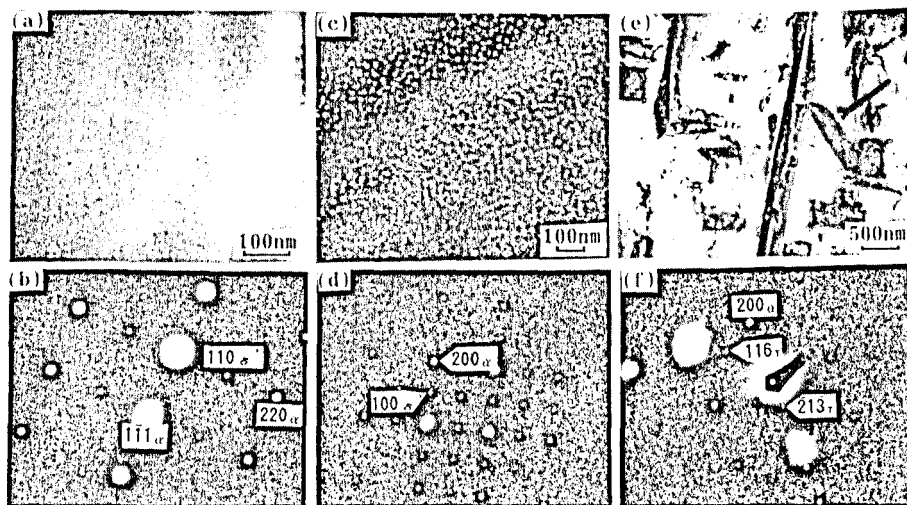


Figure 10. TEM micrographs and diffraction patterns of the Alloy II aged at 328 K for 1900 ks:(a) and (b), at 423 K for 338 ks:(c) and (d) and at 473 K for 1100 ks:(e) and (f).

In the Alloy II, the δ' and the T phases are also observed as shown in Figure 10. The shape of the δ' seems to be spherical (c) and the T seems to be thicker (e) compared with those in the Alloy I.

Diffraction patterns showed that the δ' precipitate was the metastable phase, which seems to be inconsistent with the results of S-T curve measurements. Thus, high resolution electron microscopy (HREM) was attempted to clarify the structure of the metastable phases. Figure 11 (a) and (b) are the HREM images taken on [100] axial illumination condition for the Alloy II aged at 328 K for 400 ks and aged at 473 K for 11 ks, respectively. In (a), small regions in which lattice fringes of about 0.4 nm in spacing parallel to $\{100\}_\alpha$ planes are seen. The lattice fringes appear in two crossed direction and clearly observed in few regions, while, in most regions, the fringes in one direction are faint. In the specimen aged at 473 K (b), the lattice fringes in the spherical precipitate are distinctly observed. The small regions in (a) are considered to be the precursors to δ' precipitate and cause the heat absorption B on the S-T curve, while the precipitate in (b) is the δ' phase and cause the heat absorption C.

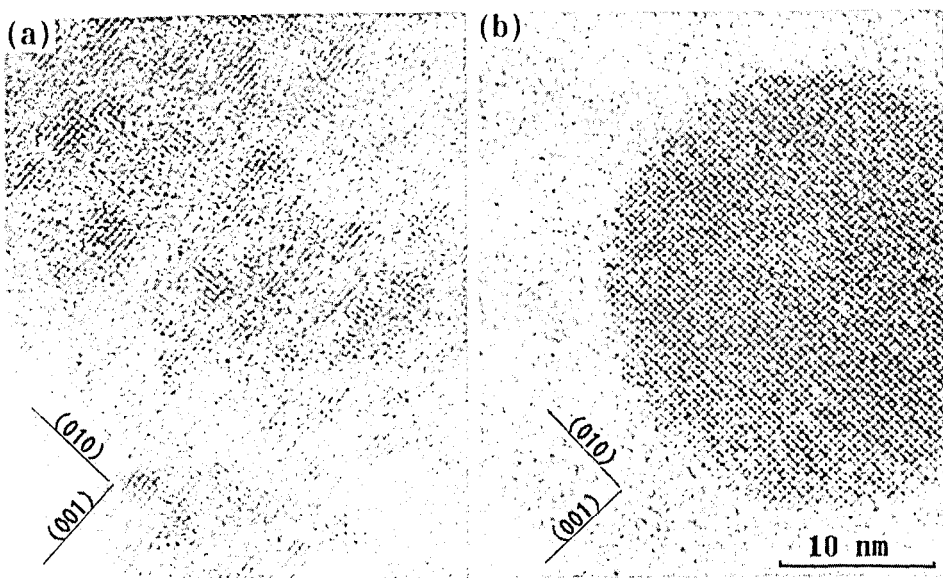


Figure 11 HREM images of the precipitate in the Alloy II aged at 328 K for 400 ks:(a) and 473 K for 11 ks:(b)

Discussion

The beginning of the second stage hardening in the Alloy I (Figure 1) is corresponding to the precipitation of T phase (Figure 5). The alloy is age-hardened by the precipitation of the T phase as well as the precipitation of

the δ' phase. The T phase precipitates as a thin plate with strain field which results in increasing the hardness, then coarsen with aging and results in decrease of the hardness. This effect of T phase on hardening is not clear in the Alloy II, because of the precipitates T in the Alloy II is rather thick which implies the lack of strain field. As a resultant, age hardnability in the Alloy II is lower than that in the Alloy I (compare Figure 1 with Figure 2). On the S-T curves, two heat absorptions B and C appear, which are considered to be due to redissolution of the metastable phases. By XRD and the electron diffraction techniques, the T phase and the δ' phase are detected. HREM study shows that there are two kinds of precipitate, both of them cause the $L1_2$ type ordered spot. Main differences on the basis of TEM observations between them are the size, shape and clearness of the ordered lattice fringes. It is known that the coherency strain between the δ' and α is low, and the interfacial energy is high due to the ordered structure of the δ' , which leads to the spherical shape of the δ' precipitate. However, in the case of the degree of order in the precipitate is low and composition of the precipitate is different from the stoichiometric value, it is not necessary to keep a spherical shape, which is considered to be the precursor to the δ' , that is, the δ'' phase proposed by Nozato and Nakai (8). The precipitation sequence in the Al-Li-Zn ternary alloy is considered as follows : super-saturated solid solution $\rightarrow \delta'' \rightarrow \delta' \rightarrow T$.

Summary

1. The precipitation sequence in the Al-Li-Zn ternary alloys is considered as follows : Supersaturated solid solution $\rightarrow \delta'' \rightarrow \delta' \rightarrow T$ phase, when δ'' is the precursor of δ' .
2. Thin plate shaped T phase precipitated on $(111)_\alpha$ contributes to age hardening.
3. The δ'' phase has $L1_2$ -like crystal structure.

References

1. W.R.D.Jones and P.P.Das, J.Inst.Metals. **88**, (1959-60), 435.
2. H.K.Hardy, ibid **84**, (1955-56), 429.
3. J.R.Pickens et al., Aluminium-Lithium, Vol.1 ed., M.Peters and P.-J.Winkler (Adenauerallee, Germany:DGM Informationsegesellschaft, 1992), 357.
4. M.J.Makin, Philos.Mag., **18**, (1968), 637.
5. L.L.Rokhlin, Ternary Alloys, Vol.6, ed., G.Petzow and G.Effenberg (Metals Park, Ohio, USA:ASM International, 1993), 403.
6. L.F.Mondolfo, Aluminum Alloys (London-Boston:Butter Worths, 1976), 559.
7. R.Nozato, H.Izawa and H.Tsubakino, J.Jpn.Inst.Met., **44**, (1980), 1203.
8. R.Nozato and G.Nakai, Trans. JIM., **18**, (1977), 679.